

Dynamic Clamp: Computer-Generated Conductances in Real Neurons

ANDREW A. SHARP, MICHAEL B. O'NEIL, L. F. ABBOTT, AND EVE MARDER

*Departments of Biology and Physics, and Center for Complex Systems,
Brandeis University, Waltham, Massachusetts 02254*

SUMMARY AND CONCLUSIONS

1. We describe a new method, the dynamic clamp, that uses a computer as an interactive tool to introduce simulated voltage and ligand mediated conductances into real neurons.

2. We simulate a γ -aminobutyric acid (GABA) response of a cultured stomatogastric ganglion neuron to illustrate that the dynamic clamp effectively introduces a conductance into the target neuron.

3. To demonstrate an artificial voltage-dependent conductance, we simulate the action of a voltage-dependent proctolin response on a neuron in the intact stomatogastric ganglion. We show that shifts in the activation curve and the maximal conductance of the response produce different effects on the target neuron.

4. The dynamic clamp is used to construct reciprocal inhibitory synapses between two stomatogastric ganglion neurons that are not coupled naturally, illustrating that this method can be used to form new networks at will.

INTRODUCTION

The electrical activity of a system of interacting neurons arises from a complex dynamic interplay between numerous voltage and ligand mediated conductances (Harris-Warrick and Marder 1991). Remarkable progress has been made in describing the properties of individual membrane conductances by using voltage and patch-clamp methods (Hille 1992). However, these methods do not provide a direct understanding of the role each conductance plays in shaping the electrical activity of a neuron or network. Pharmacological agents can be used to block individual currents to assess their role in neuronal behavior (Calabrese and DeSchutter 1992; Meer and Buchanan 1992; Tierney and Harris-Warrick 1992), but lack of specificity or lack of availability of appropriate blockers limits the utility of this method. An alternate approach, computer simulation, (Koch and Segev 1989; Marder and Selverston 1992; Traub et al. 1992) is limited by the difficulty of accurately measuring all of the currents found in all of the neurons in a biological network. Moreover, the strengths of synapses in biological networks are often difficult, if not impossible, to measure. The dynamic clamp described here offers a third and novel solution to this problem. Investigator-specified conductances are added to individual neurons or used to create artificial synapses, allowing the study of these conductances and synapses in functioning networks.

METHODS

Recordings

Cancer borealis were purchased from local (Boston, MA) fishermen. Experiments on intact stomatogastric ganglia (STGs) were

done as described in Weimann et al. (1991). Experiments on cultured neurons were done as described in Sharp et al. (1992). Physiological saline had the following composition (in mM): 440 NaCl, 11 KCl, 13 CaCl₂, 26 MgCl₂, pH 7.45. Recordings were made with single intracellular electrodes filled with 0.6 M K₂SO₄ and 20 mM KCl. The recording amplifiers (Axoclamp-2A) were used in discontinuous current clamp mode with a sampling rate of 5 kHz.

Current calculation

A membrane current (I) to be applied to a neuron is given by $I = gm^ph^q(V - E_r)$ where p and q are integers, E_r is the reversal potential of the current, and V is membrane potential. The activation and inactivation variables (Hille 1992; Hodgkin and Huxley 1952) are described by first order, nonlinear differential equations

$$\tau_m(V) \frac{dm}{dt} = m_\infty(V) - m \quad \tau_h(V) \frac{dh}{dt} = h_\infty(V) - h$$

where τ_m , τ_h , m_∞ , and h_∞ are functions of V .

Synaptic conductance

To construct a synapse we use the membrane potential of the presynaptic neuron (V_{pre}) to control the conductance of the postsynaptic neuron. The synaptic current is given by

$$I = gs(E_r - V_{post})$$

where E_r is the synaptic reversal potential and V_{post} the membrane potential of the postsynaptic neuron. The synaptic activation variable s varies between zero and one and is determined by

$$(1 - s_\infty(V_{pre}))\tau_s \frac{ds}{dt} = s_\infty(V_{pre}) - s$$

where s_∞ is given as a function of the presynaptic potential by

$$s_\infty(V_{pre}) = \tanh [(V_{pre} - V_{th})/\Delta]$$

for presynaptic potentials V_{pre} satisfying $V_{pre} > V_{th}$, otherwise $s_\infty = 0$. V_{th} and Δ are constants.

RESULTS

Artificial conductances

The properties of membrane conductances can be described by differential equations that relate the opening and closing of membrane channels to membrane potential and time. The current flowing through a given conductance can be computed if one knows the membrane potential and the reversal potential for the conductance. The dynamic clamp uses a computer to control the current injected through a microelectrode into a cell as a function of the membrane potential of the cell and properties of the conductance speci-

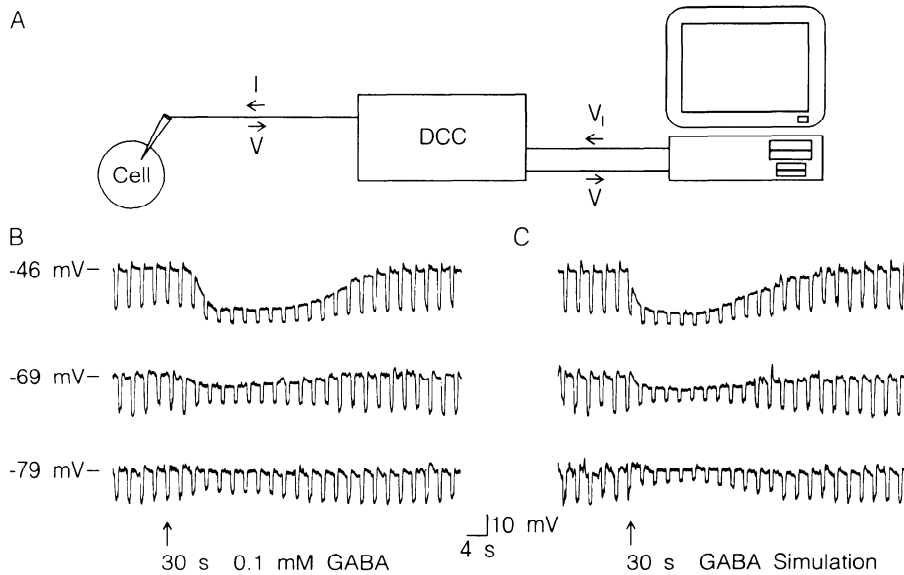


FIG. 1. Dynamic clamp. *A*: schematic of the dynamic clamp. *B*: intracellular recording from a neuron in primary cell culture dissociated from the stomatogastric ganglion (STG) of the crab, *Cancer borealis* (Sharp et al. 1992). Constant hyperpolarizing pulses (-0.05 nA) were applied every 3 s. At the upward arrow, the continuously flowing superfusion solution was changed for 30 s from control saline to 10^{-4} M γ -aminobutyric acid (GABA). This procedure was repeated at the different potentials shown. *C*: same as *B*, but the dynamic clamp was programmed to simulate a conductance change of 8 nS with a reversal potential of -75 mV. The conductance had an exponential rise ($\tau = 5$ s) and fall ($\tau = 15$ s).

fied by the investigator. The membrane potential of a dynamically clamped neuron is measured with intracellular electrodes by an Axoclamp 2A in discontinuous current-clamp mode (Fig. 1*A*). V is transmitted to the computer

through an analog-to-digital converter. On the basis of V and differential equations describing a model conductance programmed into the computer, I is computed. This is converted back into an analog voltage (V_1) and transmitted to

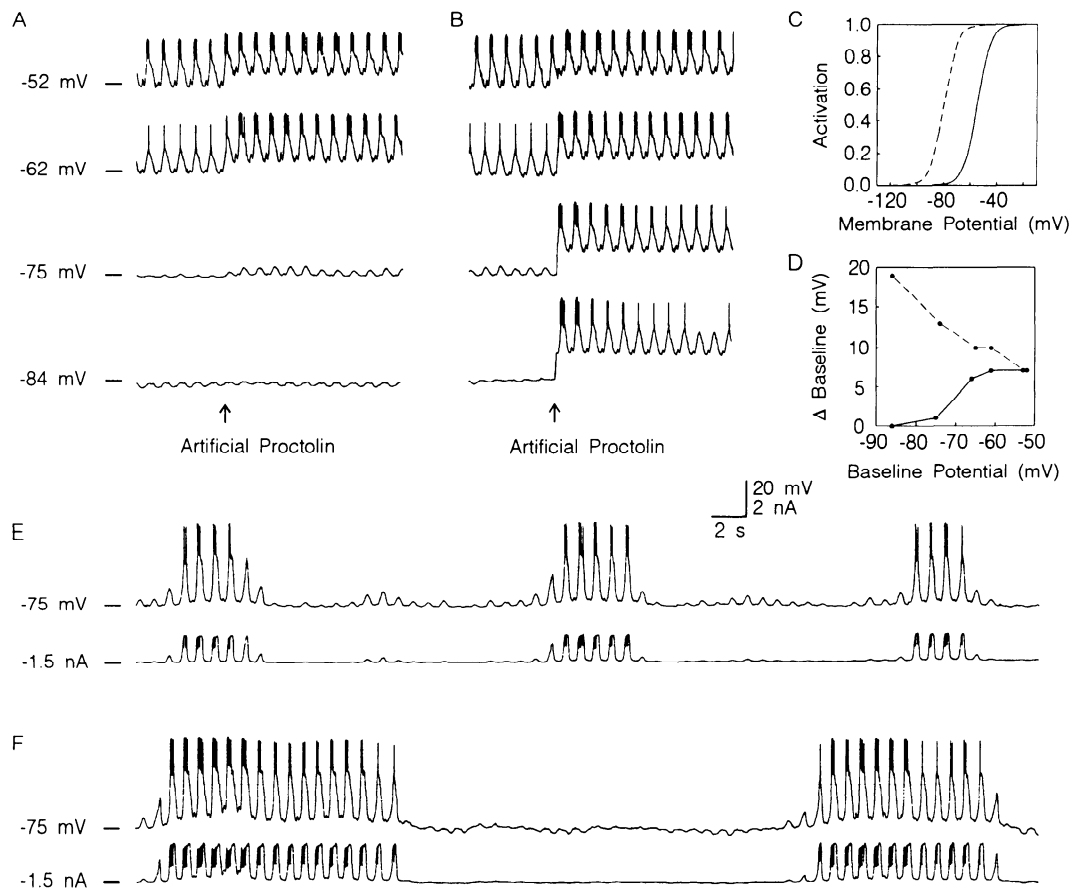


FIG. 2. Artificial proctolin response. *A*: intracellular recordings from an inferior cardiac (IC) neuron in the stomatogastric ganglion (STG) at the potentials indicated. The artificial proctolin conductance was turned on at the upward arrow ($g = 40$ nS, $E_r = -10$ mV, $\tau_m = 6$ ms). The activation curve for the proctolin current is the solid line in *C*. *B*: same as *A*, but the activation curve is the dashed line in *C*. *D*: plot of the amplitude of the proctolin response as a function of V , for the activation curve used in *A* (—) and that used in *B* (---). *E*: top is membrane potential; bottom is injected current. The neuron is hyperpolarized by the same amount as in the third trace of *A*. The proctolin conductance was 60 nS; other parameters are as in *A*. *F*: same as *E* except $g = 90$ nS.

the Axoclamp which injects the computed current into the neuron. By adjusting the parameters of the computer-implemented conductance, we control the characteristics (e.g., activation threshold, time constant, and reversal potential) of the simulated conductance.

Because the current injected by the dynamic clamp at any moment depends on the membrane potential measured at that time, this technique effectively changes the conductance of the neuron, and mimics the effects of opening real membrane channels, as illustrated in Fig. 1, *B* and *C*. In both panels, pulses of constant current were applied to a neuron to monitor its input resistance. 10^{-4} M GABA (γ -aminobutyric acid) was applied at the time indicated by the arrow in Fig. 1*B*, resulting in an increase in conductance. The GABA response was hyperpolarizing at -46 mV and showed a reversal potential of ~ -80 mV. Figure 1*C* shows the use of the dynamic clamp to mimic the GABA-activated conductance. As with the GABA application, the dynamic clamp increases the effective conductance and produces changes in membrane potential that depend on the driving force.

Some ligand-gated conductances are voltage dependent. Figure 2 illustrates the use of the dynamic clamp to simulate the voltage-dependent effect of the peptide proctolin (Golowasch and Marder 1992) on the inferior cardiac neuron (IC) of the crab STG by using the equations used in previous modeling studies (Buchholtz et al. 1992; Golowasch et al. 1992). Figure 2*A* shows the IC neuron at four different levels of steady-state current injection. The simulated proctolin conductance was applied at the upward arrow in each of the traces. Because of the voltage dependence of the proctolin conductance, this produces a substantial depolarization of the membrane potential when the neuron is at depolarized levels but relatively little effect at more hyperpolarized levels (Fig. 2*D*). If the activation threshold of the simulated proctolin conductance is changed (Fig. 2, *B* and *C*), the proctolin activated conductance now produces a depolarization throughout the voltage range illustrated (Fig. 2, *B* and *D*).

Complex phenomena can result from the interaction of a voltage-dependent noninactivating conductance (such as the proctolin conductance) with other membrane conductances (Fig. 2, *E* and *F*). The recordings in Fig. 2, *E* and *F* are at the same baseline membrane potential as trace 3 of Fig. 2*A*. In response to increasing the proctolin conductance from 40 to 60 nS (Fig. 2*E*), the cell produced periodic bouts of bursting behavior. When the proctolin conductance was further increased to 90 nS (Fig. 2*F*), the burst duration increased. The voltage dependence of the proctolin conductance is crucial for this behavior; it cannot be produced simply by depolarizing the neuron with continuous current injection (not shown). Note that increasing the proctolin current by increasing the maximal conductance produced very different effects than those produced by a negative shift in the activation curve (Fig. 2*B*).

Artificial synapses

The dynamic clamp can be used to create artificial chemical synapses between two neurons. Figure 3*A* illustrates the procedure. When the presynaptic potential crosses the

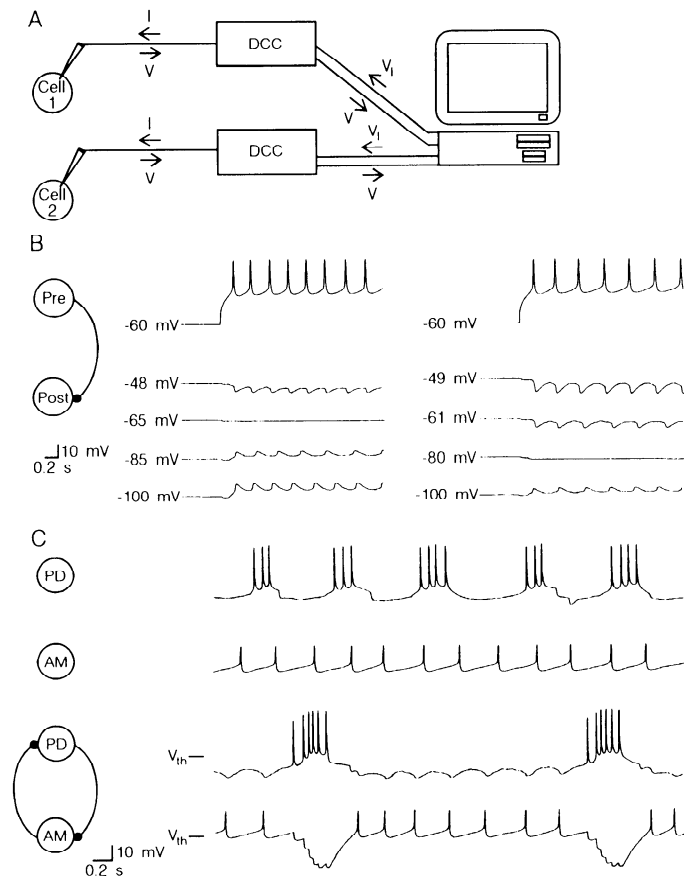


FIG. 3. Artificial chemical synapses. *A*: schematic showing the use of the dynamic clamp to construct artificial synapses. *B*: simultaneous intracellular recordings from two stomatogastric ganglion (STG) neurons. *Top*: action potentials in the presynaptic neuron evoked by depolarization; *bottom* artificial inhibitory postsynaptic potentials (IPSPs) in the postsynaptic neuron at the potentials indicated evoked by action potentials in the presynaptic neuron. *Left*: E_r is -65 mV; *right*: E_r is -80 mV. *C*: simultaneous intracellular recordings from a Pyloric Dilator (PD) neuron and an Anterior Median (AM) neuron in the STG. Under control conditions (*top*) these neurons show no synaptic interactions. *Bottom*: reciprocal inhibition established between these neurons by using the dynamic clamp (V_{th} for PD = -45 mV, V_{th} for AM = -30 mV, and for both neurons $g = 100$ nS, $E_r = -80$ mV, and $\Delta = 40$ mV).

threshold potential (V_{th}) the postsynaptic conductance is calculated as a function of the presynaptic potential and a deactivation time constant. The current injected into a follower neuron is the product of the conductance and a driving force that is the difference between the potential of the postsynaptic neuron and a reversal potential. Figure 3*B* shows artificial inhibitory postsynaptic potentials (IPSPs) evoked in a follower neuron at different membrane potentials and illustrates the effect of changing the reversal potential of the programmed IPSP.

In Fig. 3*C*, two neurons from the stomatogastric ganglion, unconnected in the control condition, were connected with artificial reciprocal inhibitory synapses. Note that the new synaptic connections result in a change in the frequency and intensity of the bursts as an emergent property of the new network.

DISCUSSION

Because the dynamic clamp creates an artificial conductance rather than injecting current (Yarom 1991), it repli-

cates accurately the way in which a current interacts with others in the cell and makes possible an array of experiments not feasible heretofore. It allows the investigator to explore, with real neurons, the role of ionic currents in shaping neuronal firing patterns. Physiological applications of modulators, such as proctolin, often result in complex changes in neural networks (Heinzel and Selverston 1988; Hooper and Marder 1987; Marder 1991). We now can ask which of those changes are a direct consequence of a single modulatory current and which may involve multiple sites of action within the network.

By using the dynamic clamp, the accuracy with which a given conductance can be simulated is equivalent to the accuracy with which the current can be measured and modeled. The utility of this method in each preparation will depend on the speed of the currents and whether there are appreciable cable effects. In many neurons the currents of interest are relatively slow, in particular those that perform modulatory roles. The dynamic clamp is particularly well suited for the analysis of these currents. Although not described at length here, the dynamic clamp can also be used, with certain limitations, to "subtract" the effect of an existing conductance in a neuron thus acting as an electronic "blocker" or "antagonist."

Analog circuits have been used previously to create artificial electrical synapses (Joyner et al. 1991; Sharp et al. 1992). We can now also form circuits with artificial chemical synapses among cultured neurons without relying on the fortuitous formation of naturally occurring synapses (Kleinfeld et al. 1990; Lukowiak 1991; Syed et al. 1990). We can modify circuits in ganglia by adding synaptic connections where they are not present. Finally, we can connect real time computer model neurons to biological neurons (LeMasson et al. 1992). The dynamic clamp makes tangible the interactions between theory and experimental work in neuroscience and should allow the exploration of the many aspects of dynamic network function not previously possible.

We thank Dr. John Rinzel for early discussions and J. McCarthy for help with manuscript preparation.

This research was supported by BNS9009251 from the National Science Foundation and MH-46742 from the National Institutes of Mental Health.

Address reprint requests to E. Marder.

Received 3 December 1992; accepted in final form 8 December 1992.

REFERENCES

- BUCHHOLTZ, F., GOLOWASCH, J., EPSTEIN, I. R., AND MARDER, E. Mathematical model of an identified stomatogastric ganglion neuron. *J. Neurophysiol.* 67: 332–340, 1992.
- CALABRESE, R. AND DESCHUTTER, E. Motor pattern generating networks in invertebrates: modeling our way toward understanding. *Trends Neurosci.* 15: 439–445, 1992.
- GOLOWASCH, J., BUCHHOLTZ, F., EPSTEIN, I. R., AND MARDER, E. Contribution of individual ionic currents to activity of a model stomatogastric ganglion neuron. *J. Neurophysiol.* 67: 341–349, 1992.
- GOLOWASCH, J. AND MARDER, E. Proctolin activates an inward current whose voltage-dependence is modified by extracellular Ca^{++} . *J. Neurosci.* 12: 810–817, 1992.
- HARRIS-WARRICK, R. M. AND MARDER, E. Modulation of neural networks for behavior. *Annu. Rev. Neurosci.* 14: 39–57, 1991.
- HEINZEL, H. G. AND SELVERSTON, A. I. Gastric mill activity in the lobster. III. The effects of proctolin on the isolated central pattern generator. *J. Neurophysiol.* 59: 566–585, 1988.
- HILLE, B. *Ionic Channels of Excitable Membranes* (2nd ed.). Sunderland, MA: Sinauer, 1992.
- HODGKIN, A. L. AND HUXLEY, A. F. A quantitative description of membrane current and its application to conduction and excitation in nerve. *J. Physiol.* 117: 500–544, 1952.
- HOOPER, S. L. AND MARDER, E. Modulation of the lobster pyloric rhythm by the peptide proctolin. *J. Neurosci.* 7: 2097–2112, 1987.
- JOYNER, R. W., SUGIWARA, H., AND TAU, R. C. Unidirectional block between isolated rabbit ventricular cells coupled by a variable resistance. *Biophys. J.* 60: 1038–1045, 1991.
- KLEINFELD, D., RACCIA-BEHLING, F., AND CHIEL, H. J. Circuits constructed from identified *Aplysia* neurons exhibit multiple patterns of persistent activity. *Biophys. J.* 57: 697–715, 1990.
- KOCH, C. AND SEGEV, I. *Methods in Neuronal Modeling*. Cambridge, MA: MIT Press, 1989.
- LEMASSON, G., RENAUD-LEMASSON, S., SHARP, A., ABBOTT, L. F., AND MARDER, E. Real time interaction between a model neuron and the crustacean stomatogastric nervous system. *Soc. Neurosci. Abstr.* 18: 1055, 1992.
- LUKOWIAK, K. Experimental reconstruction of neuronal pattern generators. *Curr. Opin. Neurobiol.* 1: 577–582, 1991.
- MARDER, E. Modifiability of pattern generation. *Curr. Opin. Neurobiol.* 1: 571–576, 1991.
- MARDER, E. AND SELVERSTON, A. I. Modelling the Stomatogastric Nervous System. In: *Dynamic Biological Networks: The Stomatogastric Nervous System*, edited by R. M. Harris-Warrick, E. Marder, A. I. Selverston, and M. Moulins. Cambridge, MA: MIT Press, 1992.
- MEER, D. P. AND BUCHANAN, J. T. Apamin reduces the late afterhyperpolarization of lamprey spinal neurons, with little effect on fictive swimming. *Neurosci. Lett.* 143: 1–4, 1992.
- SHARP, A. A., ABBOTT, L. F., AND MARDER, E. Artificial electrical synapses in oscillatory networks. *J. Neurophysiol.* 67: 1691–1694, 1992.
- SYED, N. I., BULLOCH, A. G. M., AND LUKOWIAK, K. In vitro reconstruction of the respiratory central pattern generator of the mollusk *Lymnaea*. *Science Wash. DC* 250: 282–285, 1990.
- TIERNEY, A. J. AND HARRIS-WARRICK, R. M. Physiological role of the transient potassium current in the pyloric circuit of the lobster stomatogastric ganglion. *J. Neurophysiol.* 67: 599–609, 1992.
- TRAUB, R. D., WONG, R. K. S., MILES, R., AND MICHELSON, H. A model of a CA3 hippocampal pyramidal neuron incorporating voltage-clamp data on intrinsic conductances. *J. Neurophysiol.* 66: 635–650, 1992.
- WEIMANN, J. M., MEYRAND, P., AND MARDER, E. Neurons that form multiple pattern generators: identification and multiple activity patterns of gastric/pyloric neurons in the crab stomatogastric system. *J. Neurophysiol.* 65: 111–122, 1991.
- YAROM, Y. Rhythmogenesis in a hybrid system interconnecting an olivary neuron to an analog network of coupled oscillators. *Neurosci.* 44: 263–275, 1991.